ELSEVIER

Ribosome-inactivating proteins: current status and biomedical applications

Munish Puri[1,2], Inderdeep Kaur[2], Matthew A. Perugini[3] and Raghbir C. Gupta[4]

[1] Centre for Biotechnology and Interdisciplinary Sciences (BioDeakin), Institute for Technology Research and Innovation, Deakin University, VIC 3217, Australia
[2] Protein Biotechnology Laboratory, Department of Biotechnology, Punjabi University, Patiala 147002, India
[3] Department of Biochemistry and Molecular Biology, Bio21 Molecular Science and Biotechnology Institute, The University of Melbourne, VIC 3010, Australia
[4] Department of Botany, Punjabi University, Patiala 147002, India

Ribosome-inactivating proteins (RIPs) are mainly present in plants and function to inhibit protein synthesis through the removal of adenine residues from eukaryotic ribosomal RNA (rRNA). They are broadly classified into two groups: type I and type II. Type I RIPs are a diverse family of proteins comprising a single polypeptide chain, whereas type II RIPs are heterodimeric glycoproteins comprising an A-chain (functionally equivalent to a type I RIP) linked via a disulphide bond to a B chain, mediating cell entry. In this review, we describe common type I and type II RIPs, their diverse biological functions, mechanism of cell entry, stability in plasma and antigenicity. We end with a discussion of promising applications for RIPs in biomedicine.

Introduction

Ribosome-inactivating proteins (RIPs) were first discovered in the castor oil plant, *Ricinus communis*, following the isolation and characterization of ricin [1]. However, RIPs are synthesized and widely distributed among plant genera, and have so far been found in more than 50 different species from 14 families, including the Cucurbitaceae, Euphorbiaceae, Poaceae and Caryophyllales [2]. RIPs function by irreversibly inhibiting protein synthesis through the removal of one or more adenine residues from ribosomal RNA (rRNA). RIPs are traditionally categorized into two types, referred to simply as type I and type II. Type I RIPs are single-chain proteins with a molecular weight of approximately 30 kDa, whereas type II RIPs, with an approximate molecular weight of 56–65 kDa, consist of an enzymatically active A-chain and a slightly larger B chain (a lectin subunit) with specificity for sugars exhibiting galactose-like structures [3]. Both types of RIP are localized either to plant leaves, seeds or roots. However, single-chain type I RIPs are significantly more common than their type II relatives [2]. Interestingly, type I RIPs, such as saporin, pokeweed antiviral protein and trichosanthin (TCS), are less cytotoxic than their type II counterparts, such as abrin and ricin. However, there are some type II RIPs that are non-toxic in nature [4]. The attenuated cytotoxicity of type I RIPs is the result of the absence of the cell-binding B chain [2]. Despite this cytotoxicity, type I RIPs are able to enter mammalian cells to some extent, but the precise mechanism of entry is still poorly understood. In addition to the two classic types of RIPs, a 60-kDa RIP, referred to as JIP60, has been identified from barley (*Hordeum vulgare*). JIP60 comprises an amino-terminal domain resembling type I RIPs linked to an unrelated carboxyl-terminal domain with unknown function. Thus, it is referred to as a type III RIP [5].

RIPs are ubiquitous in the plant kingdom, and abundantly present in some plant families, as mentioned above. Their role in nature is not yet completely understood, which leaves room for potential future developments. Based on existing knowledge regarding their structure, function and biological activities, RIPs from plants have potentially useful applications in agriculture and medicine. They have both antiviral and antitumor activities, which have been exploited in the preparation of immunotoxins (via antibody conjugates) by rendering the activities specifically toxic to the targeted cell [6].

Current biotechnological research into RIPs is targeted at better understanding and subsequent improvement of the cell entry mechanism, increasing specificity, reducing RIP antigenicity, prolonging their plasma half-life and understanding their role in apoptosis. These are important factors that strongly limit the application of RIPs as therapeutic agents, and are among the most

Corresponding author:. Puri, M. (munish.puri@deakin.edu.au)

1359-6446/06/$ - see front matter http://dx.doi.org/10.1016/j.drudis.2012.03.007

TABLE 1

Recently studied RIPs

Source	RIP	Molecular weight (kDa)	pI	Activity	Refs
Type I RIPs					
Amaranthus viridis	Amaranthin	30	9.8	*N*-Glycosidase, *in vitro* translational inhibition	[7]
Momordica balsamina	Balsamin	28	N/A	*N*-glycosidase, *in vitro* translational inhibition	[8]
Bougainvillea spectabilis	Bouganin	26	9.6	Adenine polynucleotide glycosylase, protein synthesis inhibition	[9]
Lychnis chalcedonica	Lychnin	≈30	N/A	Adenine polynucleotide glycosylase, protein synthesis inhibition	[9]
Momordica charantia	MAP30	30	N/A	*N*-glycosidase, anti-HIV and antitumor, cell-free translational inhibition	[10]
	α-Momorcharin	30	9	Abortifacient, antitumor and anti-HIV activity, immunosuppressive	[6]
	β-Momorcharin	29	9	Abortifacient, antitumor and anti-HIV activity, immunosuppressive	[6]
Momordica cochinchinensis	Cochinin	28	N/A	*N*-Glycosidase, antitumor activity, protein synthesis inhibition	[11]
Gelonium multiflorum	Gelonin	30	8.15	*N*-Glycosidase, antitumor activity, protein synthesis inhibition, DNase activity	[12]
Hypsizigus marmoreus	Marmorin	10	N/A	Cell free-translational inhibitory, HIV-1 reverse transcriptase inhibitory, antiproliferative activity	[13]
Lyophyllum shimeji	Lyophyllin	20	N/A	Antimitogenic, HIV-1 reverse transcriptase inhibitory, antifungal activity	[14]
Trichosanthes kirilowii	Trichosanthrin	≈13	N/A	*N*-Glycosidase, cell-free translation inhibition	[15]
Benin hispada	Hispin	21	N/A	tRNA ribonuclease, *N*-glycosidase activity, antifungal activity	[16]
Phytolacca heterotepala	Heterotepalins	28–36	8.5–9.5	Polynucleotide adenosine glycosidase activity, *N*-glycosidase activity	[17]
Flammulina velutipes	Velin	19	N/A	*N*-Glycosidase, cell-free translational inhibition	[18]
	Flammin	30	N/A	*N*-Glycosidase, cell-free translational inhibition	[18]
Type II RIPs					
Adenia lanceolata	Lanceolin	61	N/A	Polynucleotide glycosylase activity, cell-free translational inhibition, hemagglutinating	[19]
Adenia stenodactyla	Stenodactylin	63	N/A	Polynucleotide glycosylase activity, cell-free translational inhibition, hemagglutinating	[19]
Cucurbita foetissima	Foetidissimin II	61	N/A	*N*-Glycosidase, anticancer activity, cell-free protein synthesis inhibition	[20]
Sambucus ebulus	Ebulin I	56	N/A	*N*-Glycosidase, protein synthesis inhibition	[21]
Viscum album	Mistletoe	65	N/A	Antitumor activity, immunomodulatory activity, *N*-glycosidase	[22]
Viscum articulatum	Articulatin D	66	5.4	*N*-Glycosidase, hemagglutinating activity, cell-free translational inhibition	[23]
Cinnamomum camphora	Cinnamomin	61	N/A	Antitumor activity, *N*-glycosidase	[24]

active areas in current biomedical research. Accordingly, in this review, we focus on studies that have characterized the diversity, mechanism of cell entry and stability of RIPs from several plant families. We also discuss the potential biomedical applications of RIPs, including the development of a novel class of herbal-based therapeutics.

Types of RIP

Naturally occurring RIPs are found in some plant families. The highest levels of RIPs found in seeds of species from the Caryophyllaceae, Cucurbitaceae, Euphorbiaceae and Phytolaccaceae. The type I and II RIPs that have been sourced from plants are detailed in Table 1 [7–24].

Functions of RIPs

Glycosidase activity

Any protein exhibiting a glycosidase activity can be categorized as an RIP. The A ricin A-chain removes a single adenine residue from position 4324 in the 28S rRNA of rat liver ribosomes, defining RIPs as ribosome-specific *N*-glycosidases [25]. Depurination occurs on a highly conserved stem–loop structure found in the large RNA of all ribosomes. Ricin recognizes a highly conserved region in the large 28S rRNA and cleaves a specific *N*-glycosidic bond between an adenine and the nucleotide on the rRNA. The depurinated adenine is in the highly conserved sequence, GAGA, which has been shown to be important for the interaction with the ribosome-elongation factor (Fig. 1). After the removal of adenine, the deadenylated site becomes unstable and a β-elimination reaction can occur after the RNA is treated with acidic aniline, whereby the 3′ end of the rRNA is cleaved and can be detected by electrophoresis. This site is usually depicted as being present in a single-stranded loop, called the sarcin–ricin loop. It is located in domain VII, some 400 nucleotides from the 3′ end of the rRNA [1,3,6]. This particular site-specific RNA *N*-glycosidase activity is a common property of all type I and type II RIPs identified so far. RIPs from *Momordica charantia* depurinate intact ribosomes in the same manner as the ricin A-chain.

As for the A-chain of ricin, Momorcharin from *Momordica charantia* (α- and β-MMC) also deactivates eukaryotic ribosomes using a similar catalytic mechanism [26]. Another study showed that the action of α- and β-MMC on rRNA was very specific, with Momorcharins (MMCs) acting only on the 28S rRNA, but not on 18S, 5.8S and 5S rRNA, resulting in the release of a RNA fragment known as 'Endo's fragment' upon acidic aniline treatment of isolated rRNA. The *N*-glycosidase activity of the MMCs is not affected by a change in pH from 6.5 to 9.0, but enzyme activity increases with the K^+ concentration. By contrast, the enzyme activity of β-MMC fluctuates slightly with an increasing concentration of $NH4^+$ ions, whereas a significant inhibitory effect is observed with increasing Mn^{2+} concentration [6].

γ-Momorcharin also exhibits RNA *N*-glycosidase activity on ribosomes isolated from rat liver in a dose-dependent manner. To determine the action site of γ-momorcharin on 28S rRNA, the sequence of 5′-terminal nucleotides of the RNA fragment produced by γ-momorcharin and/or aniline treatment was analyzed. By comparing this nucleotide sequence with that produced by ricin,

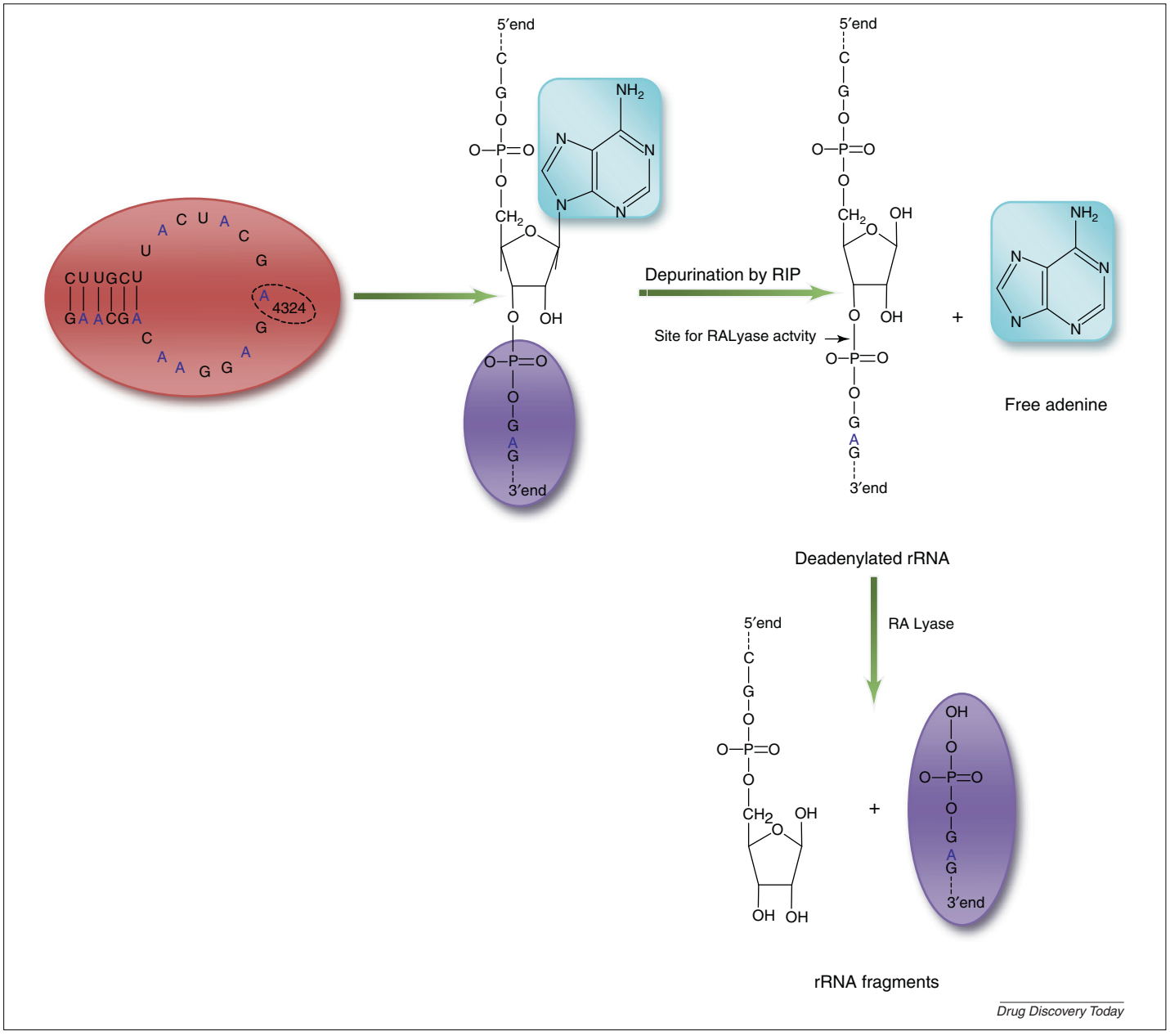

FIGURE 1

Mechanism of action of ribosome-inactivating proteins (RIPs). A specific *N*-glycosidase activity cleaves adenine (A_{4324}), which is located in the sarcin–ricin loop of the ribosomal RNA of the large subunit. The reaction product of the RNA *N*-glycosidase (deadenylated rRNA) acts as a substrate for ribosomal RNA purinic site-specific lyase (RALyase), which cleaves the phosphodiester bond at the 3′-end. The reaction products are a short (4325–4785) 3′-end fragment and a long (1–4324) 5′-fragment with a free 3′-hydroxyl terminus [2–6].

it was shown that γ-momorcharin acts on the same active site of 28S rRNA from rat liver ribosomes [6,26].

Catalytic A-chain of ricin (RAT), saporin-S6 (from *Saponaria officinalis*) and RIP from *Mirabilis expansa* (ME) (from *Mirabilis* spp.) depurinate fungal ribosomes isolated from *Rhizoctonia solani*, *Alternaria solani*, *Trichoderma reesei* and *Candida albicans*. RAT showed the strongest toxicity against the three fungal ribosomes except for that from *C. albicans*. It also showed enzymatic activity against *R. solani* and *T. reesei* at a concentration of 1 ng ml^{-1}. The enzymatic activities of saporin-S6 and ME were approximately five times and 50 times lower against *R. solani* than were those of RAT, respectively. The enzymatic activity of ME against *A. solani* ribosomes was lower than that of the other two RIPs. RAT was shown to exhibit less enzymatic activity against *C. albicans* ribosomes than against other fungal ribosomes. ME showed no depurination activity towards *T. reesei* and *C. albicans* ribosomes at a concentration up to 100 ng ml^{-1} [27]. Beetin (BE) isolated from *Beta vulgaris* depurinated both rabbit and *Vicia sativa* ribosomes, and released RNA fragments upon acid aniline treatment [28].

Inhibition of protein synthesis

RIPs from *M. charantia* were found to be potent inhibitors of protein synthesis in a cell-free system. Lectins were first detected in *M. charantia* because of their ability to inhibit protein synthesis

in Ehrlich ascites cells [6,14,29]. Lectin from *M. charantia* is the second example of a non-toxic lectin, inhibiting protein synthesis *in vitro* after *R. communis* agglutinin [1]. As for lectins, α- and β-MMCs also inhibit protein synthesis in rabbit reticulocyte cell-free lysates. The potencies (ID_{50}) of the cell-free protein synthesis inhibitory activity of α-MMC and β-MMC are reported to be as low as 0.12 nM and 0.11 nM, respectively [6].

Regarding lectins and MMCs, MAP30 exhibits a dose-dependent inhibition of a cell-free translation system. Eukaryotic translation inhibition by MAP30 was assayed in a rabbit reticulocyte lysate system and the effect on protein biosynthesis expressed as the incorporation of [^{3}H]-labeled leucine into a trichloroacetic acid (TCA) insoluble product. MAP30 exhibited cell-free translation inhibition in a dose-dependent manner with an ID_{50} of 3.3 nM [6,30]. Ribosome inactivation activity of recombinant MAP30 (rec-MAP30) was also measured by *in vitro* translation of the globin message in a rabbit reticulocyte lysate system. Rec-MAP30 exhibited a similar ID_{50} (3.3 nm) to that observed for natural MAP30 (nMAP30). Interestingly, MAP30 could not enter uninfected (normal) cells and was incapable of activating cellular ribosomes and inhibiting cellular protein synthesis in those cells [10].

γ-Momorcharin also inhibits protein synthesis in a dose-dependent manner in rabbit reticulocyte lysates with an ID_{50} of 55 nM. Compared with α-MMC, β-MMC and MAP30, the higher ID_{50} value might be attributed to the small molecular weight of this RIP [6,26]. However, the potency of δ-momorcharin is similar to that of α- and β-MMC with an IC_{50} of 0.15 nM. Contrastingly, ε-momorcharin and charantin exhibit much weaker inhibition of cell-free protein synthesis with ID_{50} values of 170 nM [6] and 400 nM [31], respectively.

Musarmins (MU 1, 2 and 3) isoforms from *Muscari armeniacum* display inhibitory activity on several cell-free systems from mammals and plants. Three isoforms of MU showed strong inhibitory activity on rabbit reticulocyte system. MU 1, 2 and 3 had IC_{50} values of 7, 9.5 and 4 ng ml^{-1}, respectively. In rat liver, IC_{50} values 79, 95 and 101 ng ml^{-1} were recorded for MU 1, 2 and 3, respectively. High concentrations of MU 1, 2 and 3 did not result in protein synthesis activity against plant-derived cell-free systems [32]. Tobacco RIP (TRIP), a single-chain RIP isolated from *Nicotiana tabacum* leaves, inhibited translation in wheat germ and rabbit reticulocyte systems. It also inhibited the wheat germ translation system more efficiently than it did the rabbit reticulocyte system. In addition, TRIP inhibited protein synthesis in a wheat germ translation system at a lower concentration and with an IC_{50} of 30 ng ml^{-1} compared with 100 ng ml^{-1} for the rabbit reticulocyte system [33]. BE inhibited protein synthesis more efficiently in rabbit reticulocyte lysates compared with in rat liver, *V. sativa* L., and *Triticum aestivum* IC_{50} values for rabbit reticulocyte lysates, rat liver, *V. sativa* L., and *T. aestivum* L. cell-free systems were 1.15, 68, 617 and 1318 ng ml^{-1}, respectively [28].

Structure–function relationship of type I RIPs

The three-dimensional structure of bouganin (from *Bougainvillea spectabilis*) and lychnin (from *Lychnis chalcedonica*) have been elucidated, along with their activities together with those of dianthin 30, PAP-R, RTA, saporin-S6 and momordin I. Relative to other RIPs, Saporin-S6 has the highest protein synthesis inhibitory activity, and efficiently deadenylates polynucleotides from rat ribosomes, poly(A) and herring sperm DNA (hsDNA). Lychnin showed little increase in protein synthesis inhibitory activity compared with bouganin. Deadenylation of poly(A) was inefficient for both lychnin and bouganin. Structure analysis of saporin-S6 revealed the presence of several exposed arginine and lysines residues surrounding the active site cleft. In lychnin, the electrostatic surface potential does not favor adenine removal. Bouganin showed some negative potential at the active site, but the negative charge of some surrounding residues prevented the enzyme–substrate interaction [6,9,14,26,49].

Antitumor activity

The RIPs from many plants have shown antitumor activity both *in vitro* and *in vivo* [34–36]. An overview of RIPs with antitumor activity is provided in Table 2. MAP30 exhibits antitumor activity against certain human tumor cell lines originating from renal, non-small cell lung and breast cancer tumors. Antitumor activity of rec-MAP30 has also been studied in several human tumor cell lines, such as brain glioblastoma, breast carcinoma, epidermoid carcinoma, liver hepatoma, melanoma, myeloma, neuroblastoma

TABLE 2

Overview of RIPs with antitumor activity

RIP	Source	Type of tumor	Study model	Refs
Type I RIP				
α-Luffin	*Luffa cylindrica*	Placental choriocarcinoma, hepatoma, breast cancer	*In vitro*	[42]
Gelonin	*Gelonium multiflorum*	Bladder cancer	*In vitro*	[44]
MAP30	*Momordica charantia*	Brain glioblastoma, breast carcinoma, epidermoid carcinoma, liver hepatoma, myeloma neuroblastoma and prostrate carcinoma	*In vitro*	[10,34,35]
MCP30	*M. charantia*	Prostrate cancer	*In vitro*	[37]
α-MMc	*M. charantia*	Lung, colon, liver, breast and epidermal cancer	*In vitro*	[38]
Pokeweed	*Phytolacca americana*	T-cell leukemia virus	*In vitro*	[36]
Saporin	*Saponaria officinalis*	Ovarian teratocarcinoma	*In vivo* (mouse)	[64]
		Prostate cancer	*In vitro*	[64]
TCS	*Trichosanthes kirilowii*	Hepatocellular carcinoma	*In vitro*	[48,65]]
Type II RIPs				
Ebulin I	*Sambucus ebulus*	Cervix epithelioid carcinoma	*In vitro*	[21]
Foetidissimin II	*Cucurbita foetidissima*	Adenocarcinoma and erythroleukemia	*In vitro*	[20]
Mistletoe	*Viscum album*	Ovarian, colorectal, renal and breast cancer	*In vitro, in vivo* (human)	[23]
Nigrin b	*Sambucus nigra*	Cervix epithelioid carcinoma	*In vitro*	[66]
Riproximin	*Ximenia americana*	Colorectal cancer	*In vivo* (rat)	[67]

and prostate carcinoma [37,38]. The antitumor activity of rec-MAP30 and nMAP30 was identical with respect to their sensitivity to particular tumor types. The most sensitive tumor cell lines were breast, central nervous system, melanoma and myeloma tumors with EC_{50} values of 0.21–0.38 nM. Prostate and epidermoid carcinomas were less responsive, with ID_{50} values of 3.42 and 1.88 nM, respectively [37].

Dexamethasone is used to treat cancers, such as Hodgkin's disease, non-Hodgkin's myeloma and lymphocytic leukemia, through inhibition of nuclear factor (NF)-κB activity [39]. Dexamethasone (1 μM) treatment of HepG2 cells does not generate an antiproliferation effect, but efficiently inhibits TCS-induced degradation of a cytoplasmic inhibiting protein (IκB-α protein) and enhanced TCS-induced apoptotic death in HepG2 cells. Dexamethasone might also inhibit dissociation of NF-κB in the cytoplasm and promote the transcription of the gene encoding IκB-α, resulting in suppression of NF-κB activation and enhanced TCS-induced antitumor effects [40].

In addition, recombinant luffin from *Luffa cylindrica* displays *in vitro* cytotoxicity against various tumor cell lines. Recombinant luffin inhibited proliferation of JEG-3 (human placental choriocarcinoma), HepG2 (human hepatoma) and MCF-7 (human breast cancer) cell lines in a dose- and time-dependent manner [41]. Tianhua (TH-R), identified from *Trichosanthes kirilowii*, was recently found to inhibit the growth of the human lung cancer A549 cell line by arresting the G0/G1 phase of the cell cycle in a dose- and time-dependent manner and inducing apoptosis [42].

Fibroblast growth factor-inducible 14 (Fn14), related to the tumor necrosis factor (TNF) receptor superfamily, has been shown to regulate a variety of cellular functions, including cell survival, cell growth, angiogenesis and inflammation. Although Fn14 is expressed at relatively low levels in normal tissues, local expression increases dramatically in injured and diseased tissue [43]. Recombinant gelonin (rGel), a type I RIP, conjugated to an anti-Fn14 monoclonal antibody (ITEM-4) was highly cytotoxic to a FN14-expressing tumor cell line. Upon administration of an immunoconjugate, ITEM-4–rGel enhanced long-term tumor growth suppression in nude mice bearing a T-24 human bladder cancer cell xenograft [44].

Antiviral activity

RIPs from *M. charantia* have broad-spectrum antiviral properties against different viruses through inhibition of viral protein synthesis in the infected cell. This, coupled with the ability of RIPs to inactivate eukaryotic ribosomes *in vitro*, suggests that the mechanism of antiviral action involves inactivation of host ribosomes in virus-infected cells [6]. Similarly, pokeweed antiviral protein (PAP) from *Phytolacca americana* exhibits antiviral activity against several viruses and also inhibits the production of the human T-cell leukemia virus I (HTLV-1). HTLV-1 is a delta retrovirus that is a causative agent of adult T-cell leukemia. It has also been associated with myelopathy and/or tropical spastic paraparesis. Currently, there is no effective antiretroviral treatment available to restrict the development of diseases associated with this virus. PAP-depurinated nucleotides within the *gag* open reading frame suppress the synthesis of viral proteins by decreasing the translational efficiency of HTLV-1 *gag/pol* mRNA [36]. Viral mRNA reduction resulting from a decrease in the viral transactivator protein, Tax, leads to feedback inhibition of transcription from the viral promoter. PAP diminishes virus production by suppressing the expression of the gene encoding HTLV-1 gene at both the translational and transcriptional levels [6].

TCS in Phase I and/or II clinical trials elicits a moderate increase in circulating CD4+ T cells and a significant decrease in p24 levels in patients with AIDS failing treatment with antiretroviral drugs, such as zidovudine [45]. TCS recognizes HIV-1 through viral envelope interactions. The viral envelope is significantly different to host cell membranes and has a rich lipid raft content and a high level of sphingolipid and cholesterol [46]. Exogenous TCS taken up by HIV-1-infected cells is associated with the lipid rafts on HIV-1 budding sites, where TCS-enriched virions are generated. TCS exploits the sorting strategy to eradicate both budding and prevent virus dissemination [47].

Studies further show that the MAP30 RIP inhibits production of the hepatitis B virus (HBV). The exposure of HepG cells to MAP30 results in inhibition of HBV DNA replication and HBsAg secretion. More specifically, MAP30 is shown to inhibit the expression of the HBV antigen, decrease viral DNA replication, downregulate replicative intermediates and reduce cDNA synthesis. High doses of MAP30 are also effective in suppressing viral replication by altering the kinetics of replicative DNA intermediates, whereas lower doses of MAP30 inhibit the expression of HBsAg and HBeAg. Thus, MAP30 inhibits the production of HBV in a dose- and time-dependent manner [48]. Luffin P1, the smallest RIP from the seeds of *L. cylindrica*, has been observed to have a potent effect on HIV replication. HIV viral replication requires assembly of a ribonucleoprotein (RNP), which comprises a Rev protein homo-oligomer and Rev response element (RRE) RNA to mediate nuclear export of unspliced viral mRNAs [46]. Rev binds to one specific site in the RRE using a 17-amino acid α-helical arginine-rich motif (ARM) for interaction with RRE. The α-helical structure of Rev ARM is important for RRE binding and the C-terminus of luffin P1 is similar to the Rev ARM. Therefore, luffin P1 might inhibit HIV-1 replication by interacting with the RRE [49].

Recent studies report the construction of several maize variants by the addition of HIV-1 protease recognition sequences to the internal inactivation region. Two maize RIP variants activated by recombinant HIV-1-infected cells inhibited viral replication in human T-lymphocytes and enhanced *N*-glycosidase activity. The first and last ten amino acids of Pro-RIP replaced with an MA/CA site and a Pro-RIP-MA/CA construct were cleaved completely by HIV-1 protease. Eleven amino acids were derived from the HIV-1 TAT-protein and fused with *N* termini of Pro-RIP and MOD to generate TAT-Pro and TAT-MOD variants. The substitution of HIV-1 protease recognition sequences (the p2/NC site and MA/CA site) generated two TAT-fused maize RIP variants: TAT-Pro-HIV-p2/NC and TAT-Pro-HIV-MA/CA. The TAT-Pro and TAT-MOD maize-RIP variant exhibited dose-dependent inhibition of HIV replication in $HIV\text{-}1_{IIIB}$ and an HIV-1 protease inhibitor-resistant virus strain. TAT-Pro had a weaker inhibiting effect on p24 antigen production and syncytium formation compared with TAT-Pro-HIV-MA/CA, TAT-Pro-HIV-p2/NC and TAT-MOD [50].

Mechanism of entry

RIPs enter the cell by first binding to cell surface receptors, then crossing the cell wall via endocytosis and finally entering the cytosol via translocation from intracellular endocytic compartments. This

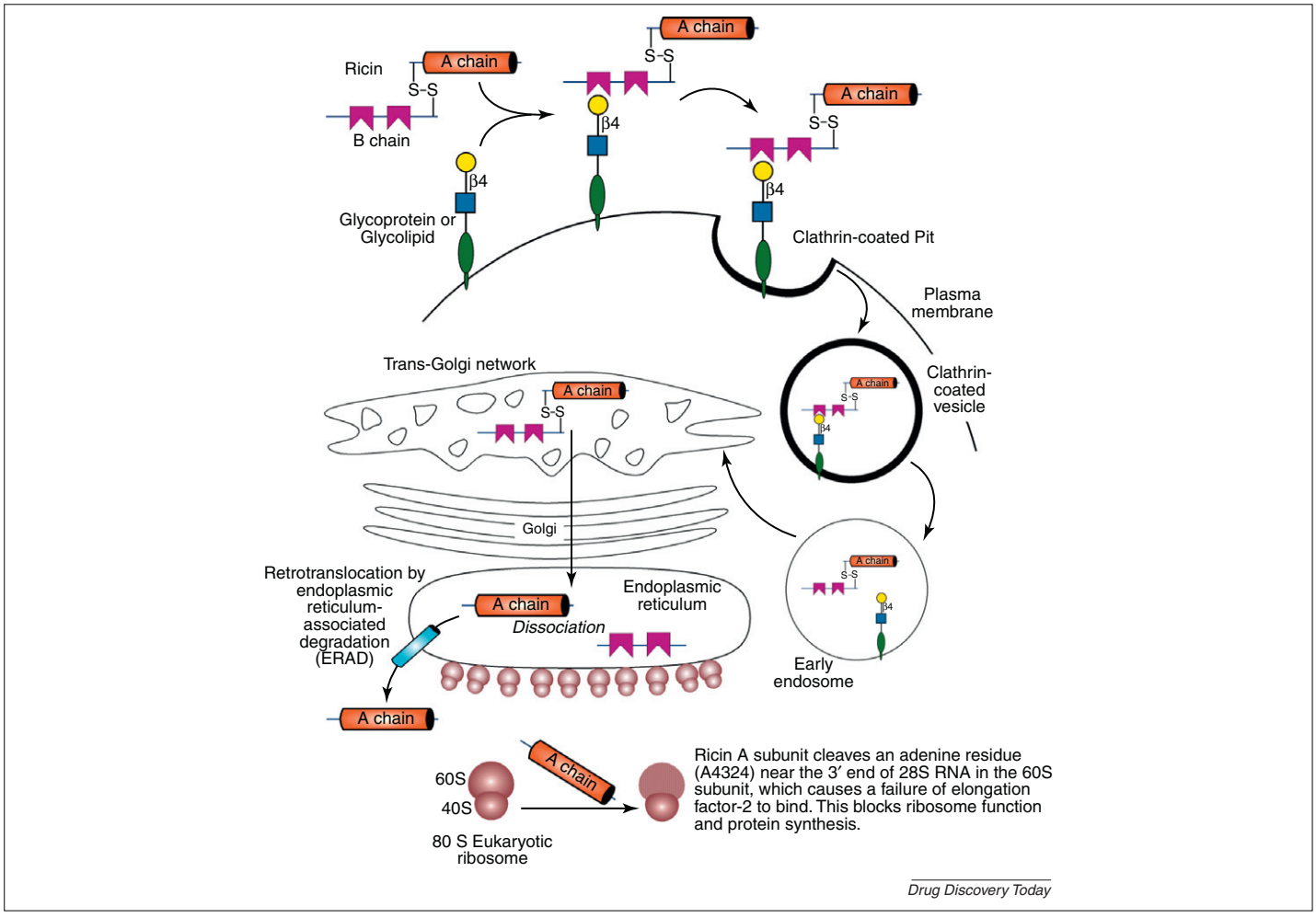

FIGURE 2

Pathway of ricin, a ribosome-inactivating protein (RIP), uptake by a cell and the putative mechanism whereby the toxic activity of the ricin A-chain in the cytoplasm results in cell death.
Modified from [56,68].

occurs after retrograde transport through the Golgi apparatus to the endoplasmic reticulum (ER) [2]. In the ER, the catalytic moieties exploit the ER-associated degradation (ERAD) pathway to reach their cytosolic targets. Most of the observations concern type II RIPs and suggest that more than one mechanism of internalization is involved. The cell–RIP interaction shows common features, including: (i) only some of the toxin molecules taken up by the cells are transferred into the cytosol and so reach their target; (ii) inhibition of protein synthesis can only be detected in cells at least 30 min after it occurred; and (iii) a single RIP molecule might be sufficient to induce cell death [5].

Internalization of type II RIPs

Ricin (a type II RIP) has evolved a mechanism for efficiently entering mammalian cells (Fig. 2). Other type II RIPs from plants are structurally and functionally equivalent to ricin, and it is assumed that their mechanism for entering target cells would be similar.

Binding to the cell surface

The first step in the cell–RIP interaction consists of RIP binding to membrane receptor sites through β-1,4 linked galactose residues, which are widely present on mammalian cell surface glycoproteins and glycolipids. The A and B-chains of ricin have mannose-containing oligosaccharide groups, which are mainly responsible for the uptake and toxicity of the toxin in rat liver kupffer and sinusoidal cells (non-parenchymal cells) [1]. However, ricin uptake by these cells is completely abolished in the presence of both galactose and mannan [51]. The binding of lanceolin and stenodactylin to cells was assessed by association with glycosylated molecules on the cell membrane through their lectin-B-chains. The presence of galactose inhibits the binding of the RIP through the lectin-B chain [52].

Endocytic uptake

Type II RIPs do not directly cross the plasma membrane, but enter the cytosol via the endocytic pathway. Ricin binds to a variety of cell surface components, where it uses different endocytic mechanisms to enter cells. Receptor-mediated endocytosis usually occurs by way of clathrin-coated pits, which are specialized depressions on the cell surface. The binding and internalization of ricin by Vero cells was first observed to use clathrin-dependent endocytosis [53]. Mannose-containing RIPs use this method of endocytosis, after being bound to mannose receptors localized in coated pits [1,6]. Unlike other cytotoxic Type II RIPs, lanceolin

and stenodactylin are internalized by mechanisms independent of clathrin-coated pits [52].

Endocytosis

The endocytic pathway comprises early and late endosomes and lysosomes. Endocytosis involves cell surface invagination of both coated and non-coated pits, leading to the formation of endosomal vacuoles. Ricin initially enters cells endocytically and is delivered to early endosomes, from where most of it is either recycled back to the cell surface or delivered via late endosomes to lysosomes, where it is proteolytically degraded. Resistance to ricin is observed when endosome-to-Golgi transport is blocked by low temperature [54]. Treating cells with ionophore monensin or Brefeldin A (BFA) compounds, which influence the Golgi morphology and function, confers resistance to Type II RIP. This suggests that the Golgi complex is required for type II RIP intoxication. Internalization can be visualized within the trans-Golgi network (TGN). Ricin binds to a variety of different surface molecules and follows various intracellular routes, one or more of which enable the toxin to be transferred into the cytosol [53]. The intracellular trafficking of lanceolin and stenodactylin is similar to that of ricin. The addition of BFA resulted in substantial protection of cells against protein synthesis induced by lanceolin and stenodactylin [52].

Transfer from Golgi apparatus to the endoplasmic reticulum

Toxins from TGN undergo retrograde transport through the Golgi stack to reach the ER lumen. Retrograde transport of ricin from the Golgi-to-ER step involves the movement via coatomer protein I (COP-I)-coated vesicles [55]. Transient expression of trans-dominant negative GTAases that regulate vesicle transport steps in the early secretory pathway partially protected cells against ricin, whereas the addition of an ER-retrieval sequence (KDEL) to the C-terminus of RTA increased the cytotoxicity of free RTA [51] and reconstituted holotoxin [1]. The RTA–KDEL interacts with Golgi-to-ER cycling KDEL receptors. The direct evidence for Golgi-to-ER transport of ricin was shown by the BFA-sensitive uptake and core glycosylation of a non-glycosylated toxin. Post-translational core glycosylation of an endocytosed protein provides evidence for the retrograde transport of ricin from the cell surface to the ER, where the oligosaccharyl transferase responsible for the core glycosylation is located [51,55].

Membrane translocation

Ricin and other type II RIPs are non-pore forming toxins, which undergo retrograde vesicular transport to the ER and into the cytosol via translocation machineries [51]. Misfolded proteins do not accumulate in the ER lumen and RTA is expelled from the ER to the cytosol. Orphan subunits that fail to become incorporated into the appropriate multimeric complexes, and aberrant proteins that are unable to assume their biologically active conformations, are detected at this stage and eliminated by proteolytic degradation. Degradation of protein in the cytosol is carried out by proteasomes. It is recognized that such proteins are exposed to the ER and proteolytically degraded in the cytosol [55], a pathway known as ER-associated protein degradation (ERAD) (Fig. 2). In the ER lumen, RTA unfolding occurs owing to its interaction with the lipid membrane; unfolded RTA then acts as an ERAD candidate, leading to its export into the cytosol [56]. Lanceolin and stenodactylin associated with cells are released into the supernatant during cellular processing and exocytosis. Unlike other type II RIPs, the percentage of non-degraded lanceolin and stenodactylin is high. Stenodactylin showed greater uptake, exocytosis and re-uptake of non-degraded RIPs [52].

Internalization of type I RIPs

Type I RIPs lack the lectin B-chain that facilitates entry and accounts for the extreme toxicity of type II RIPs. Type I RIPs are less toxic than type II RIPs, but become highly toxic if they are introduced into cells by linkage to an appropriate carrier that is capable of binding to cells. Gelonin, when conjugated with concanavalin A, demonstrates more toxicity to cells than does free gelonin [5].

Intracellular movements of saporin rely on Golgi-mediated retrograde transport to reach their retrotranslocation site. Cell surface binding of saporin is mediated by members of the low density lipid (LDL)-related family receptors and LRP-minus MEF cells, which showed a ten-times decrease in saporin sensitivity and mediated the internalization of the amino-terminal fragment (ATF)-saporin chimera through clathrin-coated pits. The Golgi complex is not a major intracellular compartment for productive trafficking of saporin compared with Vero or HeLa cells treated with BFA. However, saporin does not appear to have putative translocation domains and the cytotoxic activity of the ATF-saporin chimera is slightly increased both by chloroquine or bafilomycin A1 treatments, suggesting its passage through a putative proteolytic compartment. Saporin toxicity is not affected by treatment with BFA or chloroquine, indicating that saporin follows a Golgi-independent pathway to the cytosol and requires a low pH for membrane translocation [57].

TCS (a type-I RIP) interacts with the negatively charged phospholipid-containing monolayer under acidic conditions through hydrophobic interactions. The acidic microenvironment of the membrane changes the charges on some residues, resulting in breakage of salt bridges and charge–charge repulsion, which partially denatures TCS to a 'molten globular state' and finally leads to its membrane insertion [26]. Recent studies suggest that receptor-related protein 1 (LRP1) is an essential receptor for TCS endocytosis by JAR and BeWo choriocarcinoma cell lines that express LRP1. This might be one of the mechanisms underlying the application of TCS in the treatment of trophoblastic cancer. Choriocarcinoma cell lines significantly bind and internalize TCS that express LRP1. By contrast, HeLa cell lines have no detectable TCS binding and endocytosis. Thus, it is suggested that HeLa cells have no detectable LRP1 and an inability to bind TCS [58].

Plasma half-life of RIPs

In pharmacoproteomics and structural genomics, many newly identified bioactive proteins are generally unstable *in vivo*. To overcome this problem, RIPs need conjugation to water-soluble polymers such as polyethylene glycol (PEG). PEG is a non-toxic, non-immunogenic, non-antigenic, water soluble and US Food and Drug Administration (FDA)-approved polymer. Covalent coupling of PEG to proteins is an effective way of prolonging plasma half-life and reducing immunogenicity. This polymer has been used extensively for the modification of proteins and PEGylation conducted non-specifically through the ε-NH_4 site of lysine residue [59]. Usually, there is more than one residue (*e.g.* lysine) in a protein and its

PEGylation produces different products with variation in their structure and activity. PEGylation of proteins usually results in masking some surface sites, increasing the molecular size and enhancing steric hindrance. Therefore, attachment of PEG to proteins decreases their immunogenicity, improves the plasma half-life and stabilizes against proteolytic cleavage [60].

TCS was the first RIP found to have anti-HIV activity *in vitro*. It has limited clinical applications because of its major adverse effects, short plasma half-life, immunogenicity and neurotoxicity. TCS administration elicited production of specific antibodies *in vivo* and its re-administration resulted in a severe anaphylactic reaction leading to death. TCS plasma half-life range is 8.4–12.7 min *in vivo*. This range requires frequent administration to maintain an effective therapeutic concentration in the blood [45]. PEGylation is shown to reduce immunogenicity and prolong the circulating half-life of proteins. Specific antibodies neutralize some TCS, speed up its plasma clearance and rapidly clear glomerular filtration, which facilitates its loss via urine, all of which result in the short plasma half-life of TCS.

Further studies show that TCS has three antigenic sites: Ser (S7), Lys-173 (K173) and Gln-219 (Q219). These sites are mutated to a cysteine residue, namely S7C, K173C and Q19C. The sulfhydryl group of the newly created solitary cysteine residue of S7C, K173C and Q219C is used for PEG_{20K} attachment. PEG masks antigenic sites to prevent specific antibodies binding and so reduces antigenicity and improves plasma half-life; however, *in vitro* RIP activity is not affected. The anti-HIV activity of PEGylated TCS is retained and the longer plasma half-life can usually compensate for the reduction in activity [61].

On further investigation of PEGylated TCS, two antigenic sites of TCS; YFF81–83 and KR173–174, mutated by site-directed mutagenesis and then PEG-maleimide, were coupled with the newly created cysteine residue by site-directed PEGylation. The mean residence time (MRT) of the PEGylated TCS mutants increased 4.5–6-fold and the high-plasma clearance ($C1_p$) was reduced by approximately 50% compared with natural TCS (nTCS). The increase in molecular size of the PEGylated TCS conjugate led to reduced renal clearance, and resistance of PEGylated proteins to proteolysis contributed to the prolonged plasma half-life [62].

RIPs from bitter melon seeds were subjected to PEG modifications. Chemical modification of RIP with 20-kDa $(mPEG)_2$-Lys-NHS was performed to reduce immunogenicity by increasing the plasma half-life for *in vivo* application. The inhibitory activity of both non-PEGylated and PEGylated RIP against cancer cells, as measured by the caspase 3-assay (apoptotic pathway), is much stronger than against normal cells. The antigenicity of PEGylated RIP is reduced and plasma half-life *in vivo* increased [63].

Antigenicity of RIPs

The immunogenicity of RIPs imposes limitations on the use of these proteins as therapeutic agents. Reduction of the antigenicity of RIPs has been attempted using various approaches, including chemical modification of the proteins, such as site-specific coupling to dextran and PEG, and protein engineering. It has been observed that proteins modified by PEG are less immunogenic.

Repeated use of α-MMC can elicit an antigenic response that might neutralize its biological activity. Modification of α-MMC was undertaken to make it less antigenic while maintaining its biological activities. The three epitopic regions were determined from the three-dimensional structure of α-MMC that included the largest epitopic region from residues 71 to 136; the other two regions were from residues 1 to 14 and 195 to 222. Residues 71–136 are in close proximity to the active site and antibody binding onto these residues blocked the active site. On increasing the concentration of α-MMC, protein synthesis was inhibited; in turn, the presence of monoclonal antibody A1 blocked this inhibition [5,6,14].

TCS from *T. kirilowii* when administered to patients with AIDS induced mild to severe anaphylactic responses and neurological disorders, including myalgia, nausea, diarrhea and flu-like symptoms [45]. To reduce the adverse effects of TCS as a drug, the C-terminal domain, which contains putative antigenic sites, was systematically deleted. The C-terminus of TCS does not contain any active sites, thus deletion of the domain results in a less antigenic variant of TCS that retains its biological activities and exhibits antigenicity. In one variant of TCS, C7, the last seven amino acid residues at the C-terminus (residues 241–247) are deleted, leading to decreased antigenicity. Deletion of the whole C-terminal domain is avoided to protect the secondary structures of the domain that are required for TCS folding. The antigenicity of the C7 variant decreased by 2.7 times *in vitro* ribosome-inactivating activity, and *in vivo* cytotoxicity was ten times less than that of the wild type. Therefore, the C7 variant is a potent RIP and cytotoxin that is effective in the nanomolar range [14,26].

Further investigations showed two antigenic sites of TCS, YFF81–83 and KR173–174, that are mutated by site-directed mutagenesis. PEGylation with PEG-maleimide results in the production of three mutants. Ribosome inactivation activity of these mutants was similar to nTCS. This activity is reduced seven to ten times after conjugation to PEG-maleimide and is the result of steric hindrance of PEG on interaction between the TCS and the ribosome. Immunogenicity and toxicity decreases after site-directed mutagenesis and PEGylation, suggesting that two selected sites are located at or near the antigenic determinants of TCS. The non-specific binding and uptake of TCS by normal cells might also be suppressed by PEGylation, which shields ionic strengths [61].

Conclusions and prospects

RIPs have been used for the preparation of immunotoxins (via antibody conjugates), thus offering great potential as therapeutic agents. MAP30 has provided insight into biomedical applications of RIPs as antitumor and antiviral agents, specifically against HIV, showing great promise as an alternative therapy for AIDS. Furthermore, studies characterizing the mechanism of cell entry and intracellular trafficking of Type II RIPs have also provided insight into the therapeutic use of RIPs, including potential therapeutic roles of α-MMCs, β-MMCs and MAP30 in targeting internalized HIV in T-cells of patients with HIV. All type I RIPs investigated to date show antiviral activity against plant, fungal and animal viruses. Investigation of their interaction and transport into infected cells is required to understand their toxic effect and to find cures for the diseases caused by such viruses.

Although reported to be independent of the inhibition of cellular DNA and protein synthesis, the mechanisms through which RIPs exert their antiviral activity warrants further investigation. In such a situation, it is important to investigate the potential of RIPs in therapeutic intervention as HIV is a complex virus and

develops drug resistance at various stages of its life cycle. Importantly, further availability of structural information on RIPs could lead to the development of an entirely new range of small HIV-inhibiting molecules, which could have a significant role in combination HIV therapy. However, significant increases in the fundamental understanding of RIPs are needed to design small molecules with such therapeutic value.

Acknowledgements

The authors thank BioDeakin, ITRI, Deakin University; University of Melbourne, Australia; and Punjabi University, India; for supporting collaborative research. IK acknowledges the award of Indo-Swiss Joint Research Program (ISJRP) Scholarship. MAP acknowledges the Australian Research Council (ARC) for Future Fellowship support.

References

1 Giansanti, L. *et al*. (2010) Ricin and saporin: plant enzymes for the research and the clinics. *Curr. Chem. Biol*. 4, 99–107
2 Stirpe, F. (2004) Ribosome-inactivating proteins. *Toxicon* 44, 371–383
3 Kaur, I. *et al*. (2011) Ribosome inactivating proteins from plants inhibiting viruses. *Virol. Sin*. 26, 357–365
4 Stirpe, F. and Battelli, M.G. (2006) Ribosome-inactivating protein: progress and problems. *Cell. Mol. Life Sci*. 63, 1850–1866
5 De Virgilio, M. *et al*. (2010) Ribosome inactivating proteins: from plant defense to tumor attack. *Toxins* 2, 2699–2737
6 Puri, M. *et al*. (2009) Ribosome inactivating protein (RIPs) from *Momordica charantia* for antiviral therapy. *Curr. Mol. Med*. 9, 1080–1094
7 Kwon, S.Y. *et al*. (2001) Molecular cloning of a ribosome-inactivating protein from *Amaranthes viridis* and its expression in *E. coli*. *Mol. Cell* 10, 8–12
8 Kaur, I. *et al*. (2011) Balsamin, a novel ribosome-inactivating protein from the seeds of Balsam apple *Momordica balsamina*. *Amino Acids* http://dx.doi.org/10.10071s00726-011-1162-1
9 Fermani, S. *et al*. (2009) Structure/function studies on two type 1 ribosome inactivating proteins: bouganin and lychnin. *J. Struct. Biol*. 168, 278–287
10 Lee-Huang, S. *et al*. (1995) Anti-HIV and anti-tumor activities of recombinant MAP30 from bitter melon. *Gene* 161, 151–156
11 Cheuthong, J. *et al*. (2007) Cochinin B, a novel ribosome-inactivating protein from the seeds of *Momordica cochinchinensis*. *Biol. Pharm. Bull*. 30, 428–432
12 Li, Z. *et al*. (2007) Truncations of gelonin lead to a reduction in its cytotoxicity. *Toxicology* 231, 129–136
13 Wong, J.H. *et al*. (2008) Marmorin, a new ribosome-inactivating protein with antiproliferative and HIV-1 reverse transcriptase inhibitory activities from the mushroom *Hypsizigus marmoreus*. *Appl. Microbiol. Biotechnol*. 81, 669–674
14 Ng, T.B. *et al*. (2010) Recent progress in research on ribosome inactivating proteins. *Curr. Protein Pept. Sci*. 11, 37–53
15 Shu, S.H. *et al*. (2009) Purification and characterization of a novel ribosome-inactivating protein from seeds of *Trichosanthes kirilowii* Maxim. *Protein Expr. Purif*. 67, 120–125
16 Ng, T.B. and Parkash, A. (2002) Hispin, a novel ribosome inactivating protein with antifungal activity from hairy melon seeds. *Protein Expr. Purif*. 26, 211–217
17 Di Maro, A. *et al*. (2007) Isolation and characterization of heterotepalins, type I ribosome-inactivating proteins from *Phytolacca heterotepla* leaves. *Phytochemistry* 68, 767–776
18 Ng, T.B. and Wang, H.X. (2004) Flammin and velin: new ribosome inactivating polypeptides from the mushroom *Flammulina velutipes*. *Peptides* 25, 929–933
19 Stirpe, F. *et al*. (2007) Characterization of highly toxic type II ribosome-inactivating proteins from *Adenia lanceolata* and *Adenia stenodactyla* (Passifloraceae). *Toxicon* 50, 94–105
20 Zhang, D. and Halaweish, F.T. (2007) Isolation and characterization of ribosome-inactivating proteins from Cucurbitaceae. *Chem. Biodivers*. 4, 431–442
21 Ferreras, J.M. *et al*. (2011) Use of ribosome-inactivating proteins from *Sambucus* for the construction of immunotoxins and conjugates for cancer therapy. *Toxins* 3, 420–441
22 Pryme, I.F. *et al*. (2006) Suppression of growth of tumor cell lines *in vitro* and *in vivo* by mistletoe lectins. *Histol. Histopathol*. 21, 285–299
23 Das, M.K. *et al*. (2011) A cytotoxic type II ribosome inactivating proteins (from leafless mistletoe) lacking sugar binding activity. *Int. J. Biol. Macromol*. http://dx.doi.org/10.1016/j.ijbiomac.2011.09.006
24 He, W.J. and Liu, W.Y. (2003) Cinnamomin: a multifunctional type II ribosome-inactivating protein. *Int. J. Biochem. Cell Biol*. 35, 1021–1027
25 Tumer, N.E. and Li, X.P. (2012) Interaction of ricin and shiga toxins with ribosomes. *Curr. Top Microbiol. Immunol*. 357, 1–18
26 Fang, E.F. *et al*. (2011) Recent progress in medicinal investigations on trichosanthin and other ribosome-inactivating proteins. *Curr. Med. Chem*. 18, 4410–4417
27 Park, S.W. *et al*. (2002) Enzymatic specificity of three ribosome-inactivating proteins against fungal ribosomes, and correlation with antifungal activity. *Planta* 216, 227–234
28 Iglsias, R. *et al*. (2005) Molecular characterization and systemic induction of single-chain ribosome-inactivating proteins (RIPs) in sugar beet (*Beta vulgaris*) leaves. *J. Exp. Bot*. 56, 1675–1684
29 Xiong, S.D. *et al*. (2009) Ribosome inactivating proteins isolated from dietary bitter melon induce apoptosis and inhibit histone deacetylase selectivity in malignant prostate cancer cells. *Int. J. Cancer* 125, 774–782
30 Wang, Y.X. *et al*. (2000) Anti-HIV and anti-tumor protein MAP 30 shares similar secondary structure. *Protein Sci*. 9, 138–144
31 Parkash, A. *et al*. (2002) Purification and characterization of charantin, a napin-like ribosome inactivating peptide from bitter gourd (*Momordica charantia*) seeds. *J. Peptide Res*. 59, 197–202
32 Arias, F.J. *et al*. (2003) Musarmins: three single-chain ribosome-inactivating protein isoforms from bulbs of *Muscari armenicum* l. And Miller. *Int. J. Biochem. Cell Biol*. 35, 61–78
33 Sharma, N. *et al*. (2004) Isolation and characterization of an RIP (ribosome-inactivating protein)-like protein from tobacco with dual enzymatic activity. *Plant Physiol*. 134, 171–181
34 Lee-Huang, S. *et al*. (2000) Inhibition of MDA-MB-231 human breast tumor xenografts and HER2 expression by anti-tumor agents GAP31 and MAP30. *Anticancer Res*. 20, 653–659
35 Fan, J.M. *et al*. (2008) Effects of recombinant MAP30 on cell proliferation and apoptosis of human colorectal carcinoma LoVo cells. *Mol. Biotechnol*. 39, 79–86
36 Mansouri, S. *et al*. (2009) Suppression of human T-cell leukemia virus I gene expression by pokeweed antiviral protein. *J. Biol. Chem*. 284, 31453–31456
37 Xiong, S.D. *et al*. (2009) Ribosome-inactivating proteins isolated from dietary bitter melon induce apoptosis and inhibit histone deacetylase-1 selectively in premalignant and malignant prostrate cancer cells. *Int. J. Cancer* 125, 774–782
38 Bian, X. *et al*. (2010) PEGylation of alpha-momorcharin: synthesis and characterization of novel anti-tumor conjugates with therapeutic potential. *Biotechnol. Lett*. 32, 883–890
39 De Bosscher, K. *et al*. (2003) The interplay between the glucorticoid receptor and nuclear factor kappa B or activator protein 1: molecular mechanisms for gene repression. *Endocr. Rev*. 24, 488–522
40 Li, M. *et al*. (2010) Dexamethasone enhances trichosanthin-induced apoptosis in the HepG-2 hepatoma cell line. *Life Sci*. 86, 10–16
41 Liu, L. *et al*. (2010) Cloning and soluble expression of mature α-luffin from *Luffa cylindrica* and its anti-tumor activities *in vitro*. *Acta Biochim. Biophys. Sin*. 42, 585–592
42 Li, C-T. *et al*. (2010) The mechanism of action of Tianhua™ on anti-tumor activity in lung cancer cells. *Pharm. Biol*. 48, 1302–1309
43 Han, E.S. *et al*. (2010) Fibroblast growth factor-inducible 14 (Fn14) is expressed in the lower genital tract and may play a role in amplifying inflammation during infection. *J. Reproduct. Immunol*. 84, 16–23
44 Zhou, H. *et al*. (2011) Development and characterization of a potent immunoconjugate targeting the Fn14 receptor and solid tumor cells. *Mol. Cancer Ther*. 10, 1276–1288
45 Byers, V.S. *et al*. (1994) A phase II study of effect of addition of trichosanthin to zidovudine in patients with HIV disease and failing antiretroviral agents. *AIDS Res. Hum. Retroviruses* 10, 413–420
46 Lee, J.H. *et al*. (2008) Analysis of the EIAV Rev-responsive element (RRE) reveals a conserved RNA motif required for high affinity Rev binding in both HIV-1 and EIAV. *PLoS ONE* 3, e2272
47 Zhao, W.L. *et al*. (2009) A novel sorting strategy of trichosanthin for hijacking human immunodeficiency virus type I. *Biochem. Biophys. Res. Commun*. 384, 347–351
48 Fan, J.M. *et al*. (2009) Inhibition on hepatitis B virus *in vitro* of recombinant MAP30 from bitter melon. *Mol. Biol. Rep*. 36, 381–388

49 Ng, Y.M. *et al.* (2011) Structural characterization and anti-HIV-1 activities of arginine/glutamate-rich polypeptide Luffin P1 from the seeds of Sponge gourd (*Luffa cylindrica*). *J. Struct. Biol.* 174, 164–172

50 Law, S.K-Y. *et al.* (2010) A switch-on mechanism to activate maize ribosome-inactivating protein for targeting HIV-infected cells. *Nucleic Acids Res.* 38, 6803–6812

51 Roberts, L.M. *et al.* (2004) Ricin: the endoplasmic reticulum connection. *Toxicon* 44, 469–472

52 Battelli, M.G. *et al.* (2010) Binding and intracellular routing of the plant-toxic lectins, lanceolin and stenodactylin. *Biochim. Biophys. Acta* 1800, 1276–1282

53 Grimmer, S. *et al.* (2006) Depletion of spingiolipids facilitates endosomes to golgi transport of ricin. *Traffic* 7, 1243–1253

54 Sandvig, K. *et al.* (2010) Protein toxins from plants and bacteria: probes for intracellular transport and tools in medicine. *FEBS Lett.* 584, 2626–2634

55 Bonifacino, J.S. and Rojas, R. (2006) Retrograde transport from endosomes to the trans-golgi network. *Nat. Rev. Mol. Cell Biol.* 7, 568–579

56 Day, P.J. *et al.* (2002) Binding of ricin A chain to negatively charged phospholipid vesicles leads to protein structural changes and destabilizes the lipid bilayer. *Biochemistry* 41, 2836–2843

57 Vago, R. *et al.* (2005) Saporin and ricin A chain follow different intracellular routes to enter the cytosol of intoxicated cells. *FEBS J.* 272, 4983–4995

58 Jiao, Y. and Liu, W. (2010) Low-density lipoprotein receptor related protein 1 is an essential receptor for trichosanthin in 2 choriocarcinoma cell lines. *Biochem. Biophys. Res. Commun.* 391, 1579–1584

59 Bian, X. *et al.* (2010) Pegylation of alpha-momorcharins: synthesis and characterization of novel anti-tumor conjugates and therapeutic potential. *Biotechnol. Lett.* 32, 883–890

60 Li, M. *et al.* (2009) Antitumor activities and immunological modification of RIP from *Momordica charantia* by covalent attachment of polyethylene glycol. *Acta Biochim. Biophys. Sin.* 41, 792–799

61 Wang, J.H. *et al.* (2004) Site-directed PEGylation of trichosanthin retained its anti-HIV activity with reduced potency *in vitro*. *Biochem. Biophys. Res. Commun.* 317, 965–971

62 An, Q. *et al.* (2007) Effect of site-directed PEGylation of trichosanthin on its biological activity, immunogenicity and pharmacokinetics. *Biomol. Eng.* 24, 643–649

63 Li, M. *et al.* (2009) Anti-tumor activity and immunological modification of ribosome-inactivating protein (RIP) from *Momordica charantia* by covalent attachment of polyethylene glycol. *Acta Biochim. Biophys. Sin.* 41, 792–799

64 Kuroda, K. *et al.* (2010) Saporin toxin-conjugated monoclonal antibody targeting prostrate specific membrane antigen has potent anticancer activity. *Prostrate* 70, 1286–1294

65 Li, M. *et al.* (2010) Possible mechanisms of trichosanthin-induced apoptosis of tumor cells. *Anat. Rec.* 293, 986–992

66 Citores, L. *et al.* (2002) Targeting cancer cells with transferring conjugates containing the non-toxic type-2 ribosome inactivating proteins nigrin b or ebulin I. *Cancer Lett.* 184, 29–35

67 Voss, C. *et al.* (2006) Identification and characterization of riproximin, a new type II ribosome-inactivating protein with antineoplastic activity from *Ximenia Americana*. *FASEB J.* 20, 1194–1196

68 Varki, A. *et al.* eds (2009) *Essentials of Glycobiology*, Cold Spring Harbor Laboratory Press